Coherent Beamstrahlung at the International Linear Collider

G. Bonvicini and N. Powell

Wayne State University, Detroit MI 48201

(Dated: May 24, 2019)

Abstract

The properties of coherent beamstrahlung (CB) in the microwave part of the spectrum, as well as its usage, are introduced. Some of its features are remarkable, and they include background-free detection, passive, precision measurement of the beam-beam offset and beam length, and measurement of the ratio of the beams transverse widths.

PACS numbers: 41.85.Qg, 41.75.Ht

I. INTRODUCTION.

The problem of achieving and maintaining beam-beam collisions (BBC) at the International Linear Collider (ILC) ranks as possibly the greatest technical challenge in a project full of daunting technical challenges.

It is not difficult to see why. For the purpose of counting degrees of freedom (d.o.f.) in the BBC, each beam has an average direction in space, a charge population $N_{1,2}$, and a mean beam energy $E_{1,2}$. These eight quantities can be monitored accurately with a combination of beam position monitors and energy spectrometers. In the following, if related beam quantities are equal, the indices are dropped, i.e., $N_1 = N_2 = N$.

Next to these d.o.f, one has seven quantities, depicted in Fig. 1, that belong in the plane transverse to the beam-beam axis. These quantities are the minimum number of transverse parameters, under the hypothesis that the beams be Gaussian (GH) in both transverse dimensions. There are four transverse beam widths, one in x and one in y for each beam, plus two offsets, one in x and one in y, and one beam rotation. It is these quantities that dominate the beam-beam luminosity for a particular collision, since they specify geometrically whether two beams "hit" or "miss" each other.

Continuing the count of the degrees of freedom, one then has two beam lengths $_{z1}$ and $_{z2}$ (again under GH). The beam lengths do not enter directly in the determination of luminosity but both the beam disruption and the total radiated beamstrahlung power depend on the beam length. The beam length is famously difficult to monitor, specially in the sub-millimeter case of the ILC.

In momentum space, there are at least four angular parameters in the two beams angular distributions (under angular GH), but of particular interest is the luminosity-weighted energy distribution, $dL=dE$, which is non-Gaussian, strongly depends on beamstrahlung and significantly impacts the physics output. By measuring the beam geometrical parameters one can constrain the expectation value for the beamstrahlung yield, so that multiple BBC monitoring inevitably results in benefits other than luminosity. This paper's mostly concerns itself with the measurement of geometrical beam-beam parameters.

So, there are at least 21 degrees of freedom in the BBC under the benign assumption that the beams be exactly Gaussian in space and reasonably narrow in the energy distribution of the incoming beams. Compounding the problem, some of these d.o.f will jitter from one

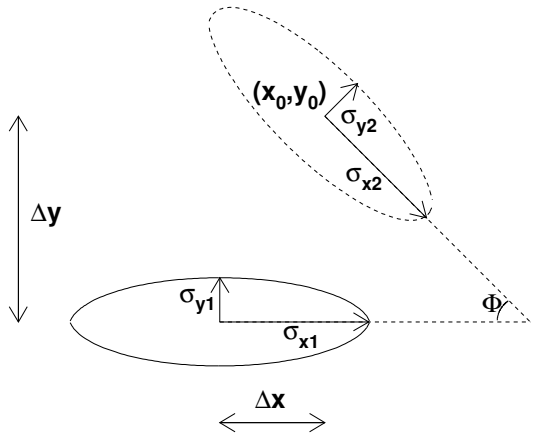

FIG. 1: The seven transverse degrees of freedom in the BBC. The beams collide in the axis of the page.

collision to the next, and all are expected to drift (to change slowly and continuously over time).

Further degrees of freedom include extra parameters specifying the beams' spatial distributions as they deviate from pure 3-D Gaussian distributions. Wakefields are expected to play a role at the ILC, and that means the beams will be transversely asymmetric with the head and the tail of the beam being different ("banana beams").

It is evident that the BBC needs to be observed in as many ways as possible. Pulse-to-pulse measurements, and passive measurements that do not require that the beams be scanned, are at a premium. Multiple measurements of the same quantity may be useful, but they will be most useful if they have different sensitivity to different beam shapes (e.g., symmetrical versus asymmetrical). The hypothesis of different sensitivities to different beam shapes for different BBC observables is likely but it has not been proven or studied so far. Measurements should be available both during the commissioning phase, when beams have a brightness perhaps 1% of nominal, and the beam-beam interaction is relatively weak.

Techniques to monitor the BBC were developed at the SLC and have been studied for the ILC. Amongst them the beam-beam deflection technique, invented by P. Bambade[1],

and recently studied by the authors of Ref.[2] in regard to a future linear collider. This technique, when used passively, is limited to the measurement of two degrees of freedom, due to Newton's Third Law equating the force exerted by each beam on the other.

The study of the high energy part of the beam strahlung spectrum would provide information about the BBC through the overall radiated power, its angular direction and spread [3] (three quantities for each beam). This technique potentially provides six d.o.f though it is unclear whether the information is completely independent. For example, all six quantities increase when the beams develop an offset in y.

In the last few years a new way to measure the BBC has been invented at Wayne State[4] and is currently under development[5] at the Cornell Electron Storage Ring, CESR. It focusses on the large angle part of the beam strahlung radiation[6]. The interest of studying that part of the radiation is that the beam strahlung polarization information can be obtained.

The device effectively provides four d.o.f on a pulse-to-pulse basis, and up to six d.o.f when the beam drift is considered[6]. The basic idea underlying the technique is that polarization is best observed at lower wavelengths, and also that one can recover 100% of the polarization information due to the special synchrotron radiation (SR) spectrum at large angles[7]. Background reduction is achieved almost entirely due to the much higher angular spread of beam strahlung, compared to the synchrotron radiation coming from the many accelerator magnets[5],[8].

Besides its many strengths, this technique has already shown itself to be one that turns on very slowly, due to its overall N^3 dependence[6]. That makes it a poor candidate to study the BBC during the ILC commissioning phase. For reasons that will become clear in a moment, this type of monitoring is termed incoherent beam strahlung (IB).

With this paper the usage of coherent beam strahlung (CB) is proposed, and its observational capabilities are discussed for the first time. This regime is dramatically different from IB because the whole beam behaves as a single particle. As shown in Sect. III, coherence sets in when one observes beam strahlung at wavelengths exceeding the beam length, AND when the beams are offset in any transverse direction. When beam strahlung is coherent, the radiation is enhanced by the factor $N \quad O(10^{10})$ which is very large.

CB is a new method with its own strengths, many of which are unlike any of the other methods. These strengths include very rapid turn-on, a large signal very nearly free of

background, the direct measurement of the two beam lengths, and the capability to measure beam-beam vertical jitter to better than 0.01 $_y$. In the past, Ref.[9] has discussed the possibility of measuring the radiation of one beam interacting with the wake field of the other beam. He termed this radiation "coherent beamstrahlung" as well, though in this paper the radiation coming from the BBC alone is considered.

Section II discusses coherent radiation in the case of synchrotron radiation in general and beamstrahlung in particular. Section III presents some simulation results. The results focus on the usage of CB during commissioning, when beams are weakest. A Table provides the CB rates for weak and nominal beams. Section IV discusses a simple method of detection and the backgrounds.

II. INCOHERENT AND COHERENT LIMIT FOR LOW ENERGY RADIATION.

Beamstrahlung is just another form of SR. Its differences with the usual kind of SR are the extremely high magnetic field B (10^5T at the ILC) and the extremely short magnet length L (0.6mm = 2 $_z$ at the ILC). The SR critical energy is directly proportional to B, so the former difference was used as the main discrimination against SR backgrounds at the SLC [10]. The latter difference is being used to discriminate against SR at CESR, because a short magnet radiates at larger angles than a long magnet[7].

This Section is qualitative in nature, for the purpose of introducing coherent beamstrahlung (as well as the lack of coherent synchrotron radiation from magnets). Quantitative results are available in the next Section. The basis of this Section is the brilliant discussion of coherence and incoherence in radiating beams, by Panofsky and Phillips[11]. That discussion is extended to show four things,

- why, in practice, coherent synchrotron radiation is never observed when a beam crosses a magnet (except for small fringe effects[2])
- why the beams need to be offset for CB to be present,
- why, in practice, CB is entirely polarized along the y axis, and
- how CB propagates in the physical environment of a vacuum beam pipe.

In Ref.[11], the spatial distribution of electrons in a ring is studied with respect to the radiation wavelength and electron multiplicity. If only one electron is present, coherent and incoherent radiation are the same. If N electrons are present, the vector potentials (which have a wave-like form) of each electron must be superposed. In practice one can also superpose the electric field vectors or the force vectors, which are the techniques adopted in this paper.

After superposition, constructive or destructive interference may arise. If electrons are forced into a highly uniform distribution, such as in a metallic wire loop, destructive interference arises and the ring will not radiate at wavelengths exceeding the electron spacing. If constructive interference is present, the radiation will be proportional to N^2.

In the case of interest here, electrons are free and they radiate because of density fluctuations in the electron bunch. The fluctuations are of order $\sqrt{N}$, and they radiate coherently, so that the radiated power $U \propto \sqrt{N}^2 = N$. The bunch radiates as the sum of the radiation intensities, and the mean radiation loss per electron is equal to that of a single electron [11]. This radiation is incoherent. If the electrons are free, incoherent radiation can not be eliminated, even when the superposition is largely destructive.

In most practical synchrotron radiation applications one is interested in the photons with wavelengths $\lambda << \sigma_z$, so that the same argument holds, that is, superposition happens within the beam and must produce incoherent radiation. That is certainly true of beamstrahlung as well. Fig. 2 illustrates how the forward waves interfere destructively, save for the aforementioned statistical fluctuations. Particle are assumed to be in phase with their radiation since their velocity differs from the speed of light by less than one part in 10^{12} at the ILC.

Consider next a bunch of length σ_z crossing a magnet of length L (this problem was already partially addressed in Ref.[8]), $\sigma_z << L$. What happens to the wavelengths $L >> \lambda > \sigma_z$? In those cases, the beam is spatially in phase with the emitted wave but emits also at a later time (Fig. 3), for example after a distance $\lambda/2$ has been covered. Again one sees that waves tend to cancel, leaving only the incoherent part. So for all wavelengths shorter than L the radiation is incoherent.

What happens in the limit $L << \lambda$ (Fig. 4)? Here radiation is truly coherent, but in practice very difficult to observe. Beam pipes have typical diameters of centimeters, and magnets have lengths of order meters. In practice these waves are absorbed in the pipe within

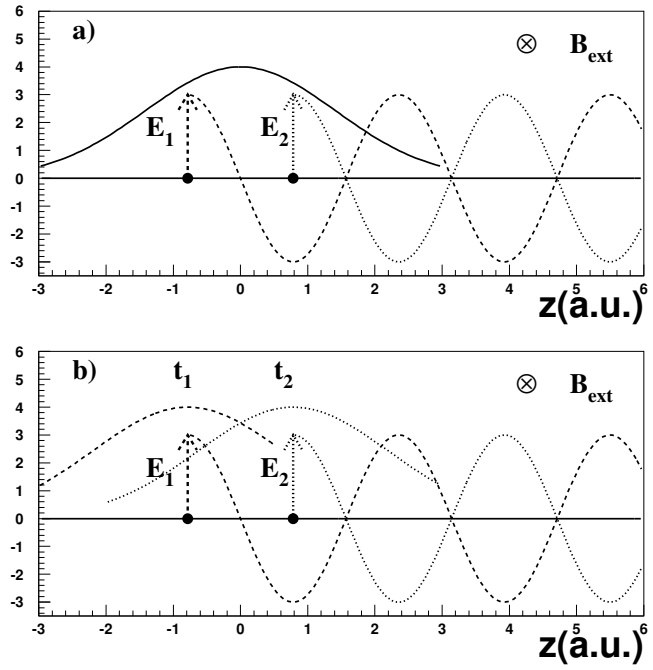

FIG. 2: Incoherent wave superposition within the bunch. a) different particles at the same time. b) same particle at different times.

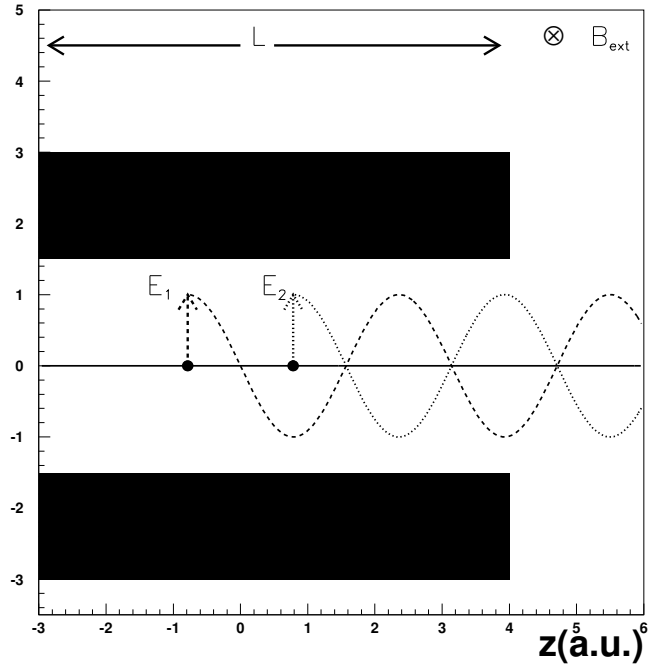

FIG. 3: Incoherent wave superposition of the bunch within a long magnet, $\quad < \quad < L$.

centimeters of the point of production and the superposition of many waves (that produces coherence) never develops. Given a beam pipe of diameter d, the microwave propagation cutoff is $= 2d$ [13]-[14]. However, for $> d$, the attenuation is typically at 0.01 dB per meter [13]-[14], so that for those frequencies microwaves can travel to a distant device and be detected.

One sees that there are constraints on the detection of coherent radiation at an accelerator. First, both the beam and the magnet have to be less than . This is not a problem for beamstrahlung, since beam and magnet (which is the other beam) have approximately the same length. Second, in practice the radiation has to propagate through a beam pipe of diameter d to a distant detector. That is possible only if $< d$. Therefore, coherent beamstrahlung can be studied if

$$d > > _z : \tag{1}$$

At the ILC, $_z = 0.3$ mm and $d = 2.5$ cm, and a large window for detection exists. We note that, with $_z$ being about 1% of d, a free radiation approximation is warranted, unlike the CESR case discussed below. This approximation will be valid for wavelengths of order of $_z$ or slightly larger. Wavelengths of order d will inevitably propagate in waveguide mode, therefore affecting to some degree the beam position monitors, as well as other instrumentation, downstream. This is a problem but not necessarily an unsolvable one. The waveguide mode will propagate more slowly than the beam itself, so that the beam induced pulse and CB could conceivably be time-resolved.

At existing accelerators, in some cases detection is impossible. For example, at the Tevatron the beams have $_z$ 0.6 meters, and the beam pipe has a diameter $d = 5$ cm. At CESR, $_z = 9$ millimeters. The beam pipe near the IP has a diameter of $d = 2.5$ cm, extending for 60 cm away from the IP. From there, the beam pipe flares out to a diameter of $d = 12.5$ cm. While close in value, waves with $< d$ should still propagate with small absorption, of the same order as the one given for the ILC. The absorption is expected to peak sharply at $= 2d = 5$ cm, due to the small piece of narrow beam pipe near the IP. It is a fact that can probably be tested experimentally if CB is studied at CESR. Clearly, in the CESR case the microwave propagation is in waveguide mode.

Finally, one builds the EM waves in the case of beamstrahlung to show how they can be coherent. First consider the situation where the beams overlap completely (a perfect

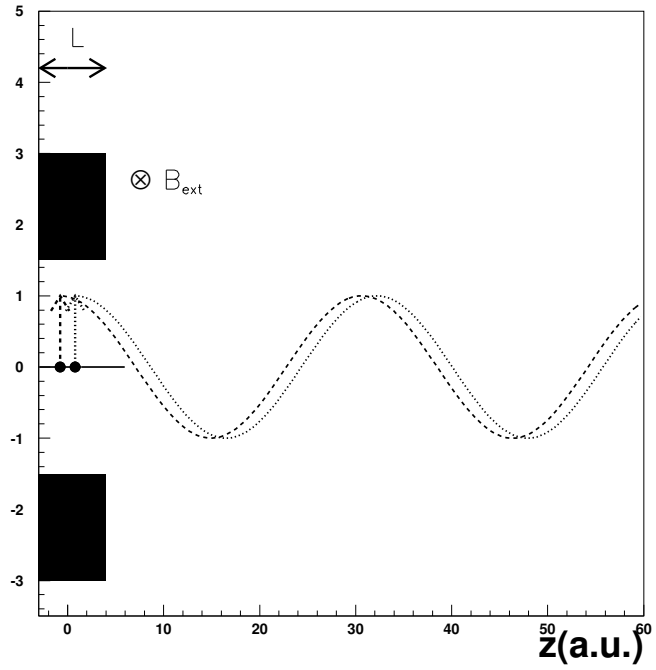

FIG. 4: Coherent wave superposition of the bunch within a magnet much shorter than the wavelength.

BBC), Fig. 5a. Four beam cells in beam 1, located symmetrically in the beam, are shown, together with the force vector components due to the attraction towards the center of the other beam. Their components cancel one another, except for statistical fluctuations. The radiation is incoherent.

In Fig. 5b the beams are offset, the x components still cancel and are incoherent, but the y components add up. Therefore, CB is present only in the case of a beam-beam offset and completely polarized in the transverse direction of offset. In practice, the ILC beams are so flat that only the y offset matters (see Table I below).

III. SIMULATIONS AND RESULTS.

In a typical beam-beam simulation, each beam is divided in many cells, and the BBC is simulated by stepping one beam through the other, one layer of cells at a time. The EM fields, in the ultrarelativistic approximation, are purely transverse so that only layers of beam 1 and beam 2 overlapping along the z-axis (the direction of motion) interact with one another. Also the ultrarelativistic limit implies that the force on a given electron in beam 1

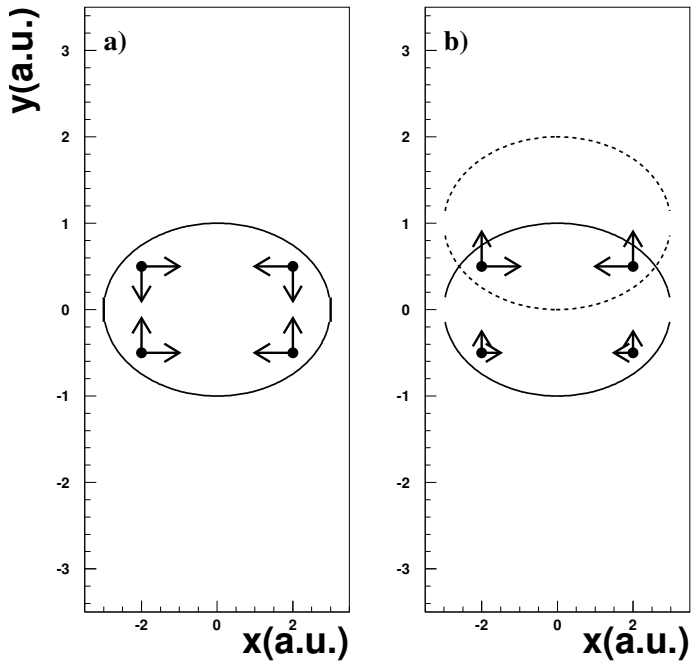

FIG. 5: a) Perfect beam-beam overlap in the transverse plane. The force vector components for four symmetrically arranged cells are shown. b) same as a), but now the beams are offset in y.

be

$$F_1 = e(E_2 + v \quad B_2) = 2eE_2:$$

Throughout this Section either the force vector or the electric field vector are used interchangeably, since they differ by a multiplicative constant. The field exerted by beam 2 on the cell i in beam 1 is computed as a sum of the fields of all the cells j of beam 2 overlapping along the beam axis

$$E_{i1} = \sum_{} E_{ij}(b_{ij});$$

with b_{ij} the transverse impact parameter between the centers of the two cells.

The field determines the deflection of the beam 1 cell for this step of the BBC, and therefore the trajectory of each cell during collision (which ultimately causes the disruption phenomenon). Dynamic quantities are now given. After some algebra, one finds

$$r'_{i1} = \frac{2N_2 r_e}{} \sum \frac{p_{j2} b_{ij}}{b_{ij}^2}; \tag{2}$$

$$F_{i1} = \frac{mc^2}{2 \ _z} \ r'_{i1}; \tag{3}$$

with the relativistic factor, m the electron mass, r_e the classical electron radius, c the speed

of light, Δ_z the step along the BBC axis, and $\Delta r'$ the (transverse) deflection during such a step. F_{i1} is the force exerted on one particle of beam 1 by the whole beam 2 layer interacting with it. The p are the fractional charge population in each cell. All beam strahlung simulation codes feature Eqs. 2-3, because they describe the way the beams disrupt one another.

When it comes to radiation, the simplest possible case is when the radiation energy loss is very small compared to the beam energy. This is the limit valid for the SLC and also for CESR today. Those cases are fairly simple to treat. Each cell's energy does not change through the interaction, and the radiated energy is proportional to the force squared. The incoherent energy vector $U(\omega)$ is formed by the two polarization components of the energy emitted at a particular frequency ω.

For beam 1 and for the particular layer under consideration is computed by summing [6]

$$U_{1x} = g \sum \quad U_{i1x} = g \frac{2N_1 r_e \Delta_z}{3\gamma^2}^2 \sum \quad p_i F_{i1x}^2; \tag{4}$$

$$U_{1y} = g \sum \quad U_{i1y} = g \frac{2N_1 r_e \Delta_z}{3\gamma^2}^2 \sum \quad p_i F_{i1y}^2: \tag{5}$$

g is a small number describing the angular and frequency acceptance of the detector. U_1 is relevant at large angle where the polarization can be 100% at certain angular locations [6]. The sum is then extended to all layers to obtain the total radiated energy for the collision. Of note are the dependence of U_1 on N_1, due to incoherence, and N_2^2, which comes through the square dependence on the force. A quantity U_0 is introduced, the energy radiated incoherently when the beams collide perfectly. If the disruption is not too large, U_0 is unpolarized, and polarization phenomena arise when the BBC is not perfect [6].

When one considers the ILC, the only change compared to CESR is that energy loss is not small compared to the beam energy. This is taken care by more complex algorithms, mainly by introducing also a set of macroparticles which are allowed to lose energy according to the quantum fluctuations. Specific simulations were done with this technique to verify the consistency of the results below.

Finally, we get to address how to simulate CB. As stated before, the radiation is assumed to propagate freely inside the beam pipe. The algorithm used in Ref. [6] is used to produce the results of Figs. 6-8, but with a change. One now adds all electric field vectors during the BBC, then squares them at the end, to evaluate coherent effects. Naming the CB power

as W, the formulae become

$$W_{1x} = g\frac{2N_1^2 r_e \ z}{3m\ c^2}^2 \Big(\quad p_i e^{ik\ x} F_{i1x})^2; \tag{6}$$

$$W_{1y} = g\frac{2N_1^2 r_e \ z}{3m\ c^2}^2 \Big(\quad p_i e^{ik\ x} F_{i1y})^2; \tag{7}$$

and likewise for W_2. As in Eqs. 4-5, the sum is run over all cells in all layers. k and x are the momentum and space photon 4-vectors. The simulation were all done assuming that the radiation propagates along the direction of motion (zero angle approximation). The coherent enhancement C shown in Figs. 6-8 is defined as $C = W = U_0$.

The approximation will hold only under the condition that the beam-beam deflection angle and the beam angular spread be much smaller than the typical angular spread of the radiation. The is probably adequate to compute the emitted power at CESR. It is almost certainly not adequate for the ILC at full luminosity, where the deflection is going to be large. If the angular divergence of the beam, including beam-beam effects, is typically $_{div}$, and the angular spread of the radiation $_{rad}$, one may reasonably expect that the coherent enhancement will remain but be reduced by a quantity of order $(_{rad} = _{div})^2$.

The algorithm's estimates of W_x, incoherent by construction, fluctuate from zero to about 10^8 of the maximum W_y. The fluctuations are due to computer roundup errors. This is irrelevant at this time, given that W_x is negligible fraction of the power output when a coherent enhancement is present (See Figs. 6-8 below). The calculation of W_y was also observed to be unstable for very small offsets. Empirically, the program was tested by running it with slightly different beam-beam offsets of, e.g., 0.499, 0.5, and 0.501_y, making sure that the results lay along a smooth curve. The program was found to be numerically stable to 1% or better when the enhancement C exceeded the number of cells in a beam (typically 30 30 40). In practice, the program does not work properly for offsets which are non zero but below $0.05\ _y$.

Table I shows the beam parameters at startup and at nominal conditions. The main simulation results are shown in Figs. 6-8 for startup ("weak") beams. In Fig. 6, the microwave power (in units of IB power) is shown for equal colliding gaussian beams as a function of the beam-beam vertical offset (in beam width units). The curves show the dependence of the coherent yield for various $ = _z$ ratios. To give an idea of the effect of energy loss (ignored in the simulations), the point with a normalized offset of 3.02 (the point with the highest C in Fig. 6) had a C of $1.376\ 10^9$ without energy loss and for $ = _z = 2$.

Beam charge N	$2 \quad 10^{10}$e
Vertical beam width $_y$	5nm
Horizontal beam width $_x$	554nm
Beam length $_z$	300 m
Beam energy	500 GeV
Beam strahlung average energy loss	5.4%
Vertical beam width $_y$	19nm
Beam charge N	$0:75 \quad 10^{10}$e
Beam strahlung average energy loss	0.1%

TABLE I: ILC nominal parameters and beam strahlung yield for each bunch crossing[15]. The quantities below the horizontal line are the "weak beam" parameters assumed to be prevalent at ILC startup. The $_{x;z}$ were assumed to be the same for weak and nominal beams.

When the energy loss was subtracted as the average energy loss for the whole cell, using the beam strahlung formulae of Ref.[17], C was $1.374 \quad 10^9$. On a scale varying over eleven orders of magnitude, 0.1% corrections can be neglected at this time.

Fig. 7 shows the side-to-side power ratio, when beams have differing lengths ($_{z2}$= $_{z1}$) = 0:8. The ordinate in this plot is the ratio of the powers emitted by the beams. The shorter beam will attain coherence at a lower wavelength than the other one, resulting in substantially more power. From the ratio, and its dependence on wavelength, one measures accurately the two beam lengths (with a precision which is probably dominated by uncertainties in the wavelength being detected).

Fig. 8 shows the same plot as Fig. 6, for beams which have different beam widths ($_{y2}$= $_{y1}$ = 3). The slower turn-on of the coherence curve of the wider beam is noted. Clearly CB measures two distinct degrees of freedom, which are, roughly speaking but not exactly, the ratio of the beam-beam offset and the vertical width of each beam.

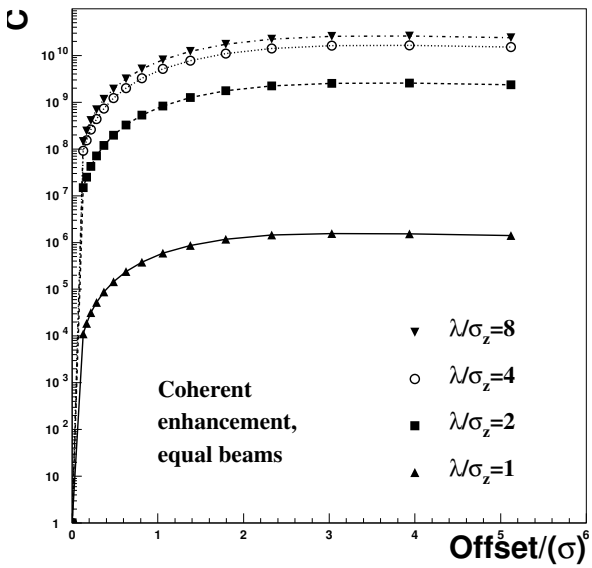

FIG. 6: CB yield as a function of the beam-beam offset. The simulations were done with ILC "weak beam" conditions, Table I ($N = 0.75 \quad 10^{10}$; $_y = 19$nm). Plots are shown for four different wavelength-beam length ratios. The markers locate the points where the simulation was performed.

IV. DETECTION OF COHERENT BEAM STRAHLUNG AT THE ILC.

It has been already noted that CB has huge fluctuations for relatively small changes in offset, and that the radiation of interest (between 0.3 and 1 mm wavelength) will travel unimpeded inside the ILC beam pipe. It was also noted that the offset is measured by the CB power, that the beam length is measured as a ratio of powers at different wavelengths, and that the ratio of transverse widths is observed through the ratio $W_1=W_2$ (or alternatively $C_1=C_2$).

It was also noted, in Fig. 6, that one will be able to measure sub-nanometer jitter at the ILC, even when the beams are tens of nanometers wide. CB jumps by orders of magnitudes for relatively small changes of offset. Assuming a 5% measurement of W, and initial beams of 20-40 nanometers, one can see that CB will be sensitive to jitter below 0.1-0.2 nm. Thus diagnostic (and remediation) of some of the most worrisome instabilities of the ILC can start long before the beams are made small, possibly improving the efficiency of the whole ILC project.

In this Section the problem of detection is addressed, but also some ideas are given on how to handle the potentially large power of CB. The microwave radiation under consideration has a typical angular spread of 0.1 mrad with respect to the electron instantaneous direction (estimated using the large angle synchrotron radiation formulae of Ref. [7]). The angular spread does not depend on whether the radiation is coherent or incoherent, as long as the observation angle is such that $<< {}_z =$, which is clearly the case here. 0.1 mrad is less than the angular spread due to the typical beam-beam deflection, which is 2-3 mrad at nominal conditions. The microwave beamstrahlung image at 100 meters will be of order 8-12 cm (assuming a 95% contour of the image) and forming a pixel image is an interesting possibility, and possibly the topic of a future paper.

In Table II the expected yields for coherent beamstrahlung at the ILC are listed. They are very large of course, because the beam populations are of order 10^{10}. The maximum instantaneous maximum power is larger by a factor of $4 \quad 10^7$. The average power for the ILC at full luminosity is given as a range only, due to the same-angle approximation discussed in Section III. The average power emitted in the microwave region will probably exceed 1kW when full strength ILC beams are offset by a few ${}_y$, and this number is to be compared

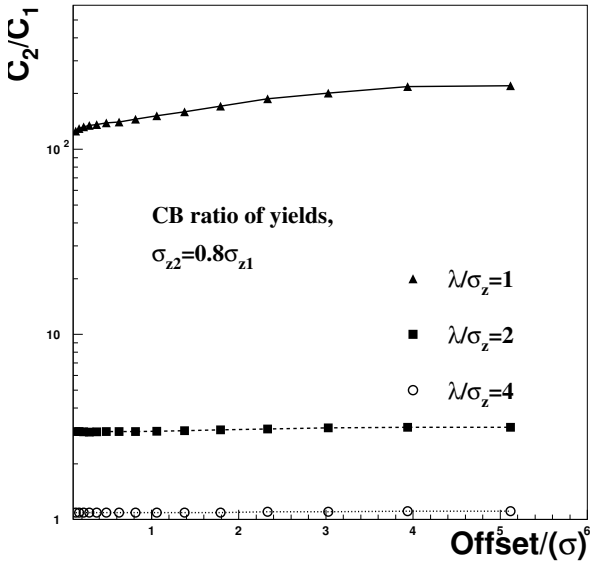

FIG. 7: CB ratio of yields (beam 1 versus beam 2) as a function of the beam-beam offset. The simulations conditions are described in Fig. 6, but ${}_{z2} = 88$ m.

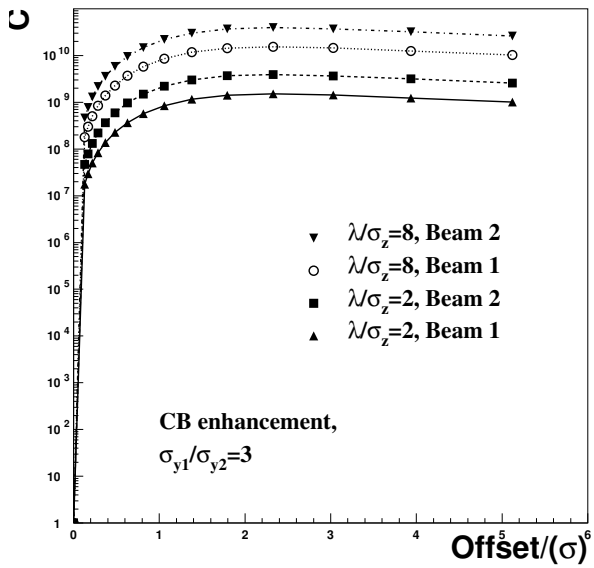

FIG. 8: Same as Fig. 6, but $_{y1}$ = 57nm .

with about 1MW in incoherent beamstrahlung.

A possible concern is that coherent beamstrahlung will blind a lot of equipment downstream whenever one of the beams jumps by a few $_{y}$. This concern has been partially addressed in Section III in regard to the part of the spectrum that propagates in waveguide mode, but also the free radiation (which is on time with the beam) needs to be addressed. It is suggested here that the beam dump window be as reflective as possible and tilted so as to bounce the microwave burst to another beam dump, leaving only the CB detector in harm way (Fig. 9 below). The need for the window to be a very good mirror is stressed here, because all microwave power will be deposited very close to the surface. Mechanical resonances of the window, that may have a period which is a multiple of the bunch-bunch period, are probably not a problem. The maximum impulse on the window (derived from Table II) is a modest 4X10^{8} N sec for a single bunch crossing.

The backgrounds from the machine magnets can be estimated. In the low frequency limit, one can use classical synchrotron radiation formulae which are accurate up to the beamstrahlung fraction energy loss. The total incoherent energy U in a given low photon

Nominal conditions, zero offset	17 W 46 nW
Nominal conditions, 3 offset	1 to 200kW 2 to 400W
Startup conditions, zero offset	1 W 2.4nW
Startup conditions, 3 offset	40W to 4kW 0.1 to 10W

TABLE II: Microwave beam strahlung average power for nominal and startup conditions. For each condition, the first power is for all wavelengths in excess of 0.3mm, the second for 0.9mm with a 0.7% bandwidth.

frequency window ! for a magnet of length L and magnetic field B is[3]

$$U \quad \frac{P_0 L}{c}\left(\frac{!}{!_c}\right)^{1=3}\frac{!}{!_c};$$

with $!_c$ being the critical frequency. Replacing the magnetic field dependence for P_0 / B^2 and $!_c / B$, one finds

$$U / B^{2=3}L; \tag{8}$$

which provides a simple way to compare the intensities of two different SR. The B of an ILC beam is of order 10^5 Tesla, and its length is 2 $_z$. For the backgrounds one assumes approximately 100 meters of magnets with an average B 3T.

By comparing the two estimates according to Eq. 8, for incoherent beam strahlung signal and magnets background, one sees that the incoherent beam strahlung radiation will be approximately 5% of the magnets background. An offset of 0.1 $_y$ should be sufficient to take the CB well above background. The machine background, as estimated here, is probably too low to be detected by the device sketched below.

Given the large power and relatively small angular distribution a detection device is not difficult to design. The apparent challenges are how to safely extract the microwave beam out of the powerful beam strahlung spray, and how to accomodate the huge dynamic range exhibited in Fig. 6. The results of Figs 6-8 suggest three or more different bands. These are assumed to be centered at 0.3, 0.6 and 0.9 millimeters (each band having a 0.7% width,

see below). Strictly speaking this part of the spectrum is still in the far infrared, however, detection techniques similar to the microwave region apply.

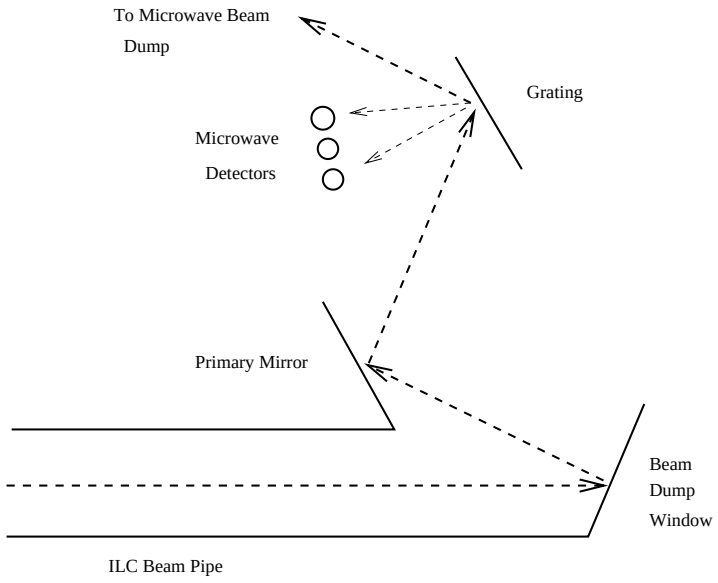

FIG. 9: Basic CB detection: a) reflection off slightly tilted beam dump window; b) extraction by a primary mirror at 15 meters; c) angular spreading by a microwave grating; d) detection by three microwave diode arrays.

Given the presence of many machine components vying for space, and RF noise from the nearby beam, one wishes to build this device as far away as possible from the beam line. We consider the beam dump window, which will function as the primary mirror, to be tilted by one degree (17 mrad) from its optimal orientation (Fig. 9). This arrangement increases the amount of radiation and heat deposited in the window by beamstrahlung by approximately 0.03%. This may look like one more aggravation for beam dump designers. Very possibly there is no choice except to do build the window at an angle, because such a strong microwave beam should simply not be reflected back into the ILC.

The window reflected microwave beam (and all other wavelengths all the way to near UV) is collected about 15 meters in front of the beam dump, approximately 26 cm from the beam line. Fig. 9 shows a primary mirror that bounces the radiation away from the beam line. The window and the primary mirror need not be polished, in fact the typical roughness of beam pipe metal (typically a few microns) would be useful to disperse unwanted shorter

wavelengths. At the same time these "mirrors" would reflect microwaves perfectly, being at least $\lambda/20$ smooth.

The third mirror is in fact a grating. Such a device (assumed to have an area of 30 × 30 cm^2) can be easily manufactured out of 143 razor blades spaced by $D = 2.1mm$. The interest of using razor blades is that their edge will be well above (perhaps one inch) the blades support. Radiation whose $\lambda << D$ will not scatter and be absorbed in the non-reflective background behind the blades (which will act as another beam dump and be also water cooled). The radiation whose $\lambda >> D$ which was not absorbed by the grid can not have secondary maxima, will see the grating as a good mirror, and reflect the rest of the radiation to the final microwave beam dump.

This grating effectively acts like a broadband filter, leaving only the band of interest being reflected at an angle by the grating. The grating will have a wavelength resolution of order 1/143, or 0.7%. This number will reflect into a measurement of σ_z which should be of the same order.

Radiation in each of the three bands is then collected at their first order maximum (respectively at 12, 25 and 40 degrees with respect to the main reflected microwave beam) by three microwave detector arrays. These are in danger of failure due to the spikes in microwave radiation they may receive. However, one notices that the arrangement allows a power reduction of close to three orders of magnitude compared to the entire signal.

A microwave filter (water cooled) is located in front of the second and third array to prevent, for example, the second order maximum of 0.45mm radiation from introducing a spurious signal in the 0.9mm detector.

The choice of detector is restricted to two candidates. One candidate is the traditional tunnel diode, as sold by Eclipse[18]. This diode is far superior, for this application, to the most common microwave Schottky diode. First, it is much faster, 10nsec typical rise time against a few hundred nsec. Second, it has a very large dynamic range, about 40dB from noise to maximum output. Third, the V-I curve flattens at high voltages, effectively limiting the power in the diode and helping minimize diode failure. The nominal sensitivity of these diodes is around 1V/mW.

The second candidate consists of heterodyne detectors[19]. These have been developed relatively more recently and can resolve picosecond signals. It is unclear whether they can provide the dynamic range that is required here, however, being more sensitive than tunnel

diodes, they could eventually be part of the detection device. In the following we assume a tunnel diode system, based on their desirable V-I curve, large dynamic range, and reasonably fast rise-time.

Ideally one could have two diodes, side by side, covering the same solid angle but masked by attenuators of different strength (given the numbers of Table II, 20dB and 50dB). The strongest attenuators are really needed only for the longest wavelengths, as Fig. 6 shows, because shorter wavelengths span a more modest dynamic range. Most probably, it will be desirable to extract the microwave beam outside the vacuum (diamond, quartz or amorphous silicon are transparent in this band) so as to replace failing diodes easily.

In each array, all diodes will be connected to the same power supply, and control of the biasing voltage can give close to two orders of magnitude control of the output current. In practice the diodes voltage will be decreased as the ILC ramps up. All diodes are properly gated and connected to their own fast ADC. From there the data enter the ILC data stream.

This simple arrangement would effectively provide a dynamic range of 10^8, which should easily cover the expected signal from 0.2 offsets at startup to the maximum expected signal at nominal conditions.

The diodes are also quite small (millimeters in size). The size of each microwave detector, in fact, is determined by the size of the attenuator or filter (which typically has the diameter of a BNC connector), so that several detectors should be able to fit within the same device.

This is a most basic design for the device, but one that should provide the information promised by Figs. 6-8. Future detector development could include the polarization splitting of the microwave signal (the x component would give the offset in x), and the projection of the microwave image onto a matrix of diodes for the purpose of imaging the BBC. Adoption of logarithmic electronics should simplify the dynamic range problem. The option of developing a fast, low sensitivity (perhaps 1 V/W) device with a V I curve asymptotically going to zero would also assure that the detectors would not fail during protracted data taking.

V. CONCLUSIONS.

It appears that coherent beam strahlung has a role to play at the ILC, its observables being somewhat different from more established beam-beam monitoring methods. While

CB manifests itself only when the beams are offset, beam jitter should provide enough collisions, where the signal is usable, to continuously monitor the beams.

The strength of the method include large, background-free signals, which allow measurements of the BBC as soon as the ILC turns on, direct measurements of the beam-beam offset, probably to an incredible precision well below 1nm, their respective beam lengths, probably to 1% or better precision, and the ratio of their transverse widths.

There is much left to do about coherent beam strahlung. The exact coherent enhancement in the presence of a large angular divergence, its exact transmission mode down the beam pipe, the possibility of imaging the BBC through coherent beam strahlung, all have to be assessed.

Discussions with N. Delerue, G. Dunifer, L. Favro and F. Villa are gratefully acknowledged. This work was supported by NSF grants NSF-PHY-0113556, NSF-PHY-0116058 and NSF-PHY-0101649, and DOE grant DOE-FG02-04ER41.

---

[1] P. Bambade, SLAC-CN-303

[2] O. Napoly and D. Schulte, DESY-TESLA-2001-15.

[3] N. Delerue and T. Tauchi (KEK, Tsukuba), physics/0408132.

[4] G. Bonvicini and J. Welch, Nucl. Inst. and Meth. 418, 223, 1998.

[5] N. Detgen et al., CBN-99-26.

[6] G. Bonvicini, D. Cinabro and E. Luckwald, Phys. Rev. E 59: 4584, 1999.

[7] R. Coisson, Phys. Rev. A 20, 524, 1979.

[8] G. Bonvicini, CBN-98-12.

[9] Jing Shen, BIHEP-DE-93-03.

[10] G. Bonvicini et al., Phys. Rev. Lett. 62: 2381, 1989.

[11] W. Panofsky and M. Phillips, "Classical Electromagnetism", Addison-Wesley Ed., page 370.

[12] R. Bossart et al., Nucl. Instrum. Meth. 164: 375-380, 1979.

[13] J.D. Jackson, "Classical Electrodynamics", 2nd Edition, Wiley Ed., Chapters 8 and 14.

[14] H.H. Skilling, "Fundamentals of Electric waves", 2nd Edition, John Wiley and Sons, Chapter XIII.

[15] http://lcdev.kek.jp/ILCWS/Talks/15wg1-2-ILC.pdf

[16] http://www-sldnt.slac.stanford.edu/nlc/confgs/2002/index.html

[17] M. Jacob, Tai Tsun Wu, and G. Zobernig, Z. Phys. C 53: 479-484, 1992.

[18] http://www.eclipsemicrowave.com/

[19] For two possible accelerator physics applications of heterodyne detectors, see T. Kotseroglou et al., SLAC-PUB-7511; T. Shintake, KEK-PREPRINT-96-81.